Available online at www.sciencedirect.com
SCIENCE DIRECT®

Journal of the European Ceramic Society 23 (2003) 1329–1335
www.elsevier.com/locate/jeurceramsoc

Microstructure and dielectric properties of strontium barium niobate ceramics synthesized by partial coprecipitation

P.K. Patro[a], A.R. Kulkarni[a,*], C.S. Harendranath[b]

[a]*Department of Metallurgical Engineering and Materials Science, Indian Institute of Technology, Bombay Mumbai-400 076, India*
[b]*Regional Sophisticated Instrumentation Centre, Indian Institute of Technology, Bombay Mumbai-400 076, India*

Received 21 May 2002; received in revised form 31 July 2002; accepted 7 August 2002

Abstract

Strontium Barium Niobate, $Sr_{0.5}Ba_{0.5}Nb_2O_6$ (SBN50), has been synthesized, for the first time, by partial coprecipitation of $SrCl_2$ and $BaCl_2$ on Nb_2O_5. Powder X-ray diffraction study shows tetragonal tungsten bronze phase formation at 1200 °C. Particle morphology and size of calcined powder has been examined using Transmission Electron Microscopy. The particle size of calcined powder ranges between 250 and 300 nm. The green compacts have been sintered at 1250, 1300 and 1350 °C and at each temperature for 6, 12 and 24 h, respectively. Effect of sintering time and temperature on dielectric properties has been investigated. Scanning electron microscopy has been used for grain morphology studies. Grains have been found to be tetragonal in shape and show variation in size for different sintering conditions. Highest dielectric constant (ε) has been observed for the pellet sintered at 1350 °C for 6 h. A variation in T_c from 93 to 119 °C has also been observed.

Keywords: Dielectric properties; Grain size; Powders-chemical preparation; Sintering; $(Sr,Ba)Nb_2O_6$

1. Introduction

Tungsten bronze structured Strontium Barium Niobate, $Sr_{1-x}Ba_xNb_2O_6$ (SBN), a solid solution of $SrNb_2O_6$ and $BaNb_2O_6$ with $x = 0.25$–0.75, has received attention because of its wide applicability.[1] It finds applications largely in electro-optic,[2,3] piezoelectric[4] and surface acoustic wave (SAW) devices[5] owing to its large pyroelectric coefficient[6] and photorefractrive properties.[7,8] In addition, the unique feature of SBN is that it facilitates to obtain tailor made materials with desired Curie temperature, ferroelectric properties, dielectric constant and microstructures by changing the composition.[6,9]

SBN has been reported to have been synthesized using various methods and with different Sr:Ba ratio. For example, in single crystal form by Czocharlski method,[7] in polycrystalline form by solid-state reaction synthesis,[10–12] from sol-gel route,[13,14] hydrolysis aging[15] and from EDTA complex chemical route.[16] Although the aforementioned methods help in realizing some desirable properties in SBN, they have some inherent disadvantages like extensive grinding steps, inhomogeneity, moisture sensitivity of precursors, synthesis of precursors, etc. Although coprecipitation method has been used for preparing many ceramic materials with fine grained and uniform microstructure, it has so far not been applied to SBN.

In the present work, coprecipitation method has been adopted for the first time for the preparation of SBN50. $SrCl_2$ and $BaCl_2$ were precipitated on Nb_2O_5. Ammonium carbonate was used as precipitant. The coprecipitation of this type has been termed here as partial coprecipitation since one of the components of the three components is in solid state, i.e. dispersed Nb_2O_5 particles. The effect of sintering parameters, temperature and time of sintering, on microstructure and the dielectric properties is investigated.

2. Experimental details

Starting materials; 99% $SrCl_2.6H_2O$ (Loba Chemicals, India), 99% $BaCl_2.2H_2O$ (Ranbaxy Chemicals, India) and 99.95% Nb_2O_5 (Spectrochem, India) were

* Corresponding author. Tel.: +91-22-576-7636; fax: +91-22-572-3480.
E-mail address: ajit.kulkarni@iitb.ac.in (A.R. Kulkarni).

0955-2219/03/$ - see front matter © 2002 Published by Elsevier Science Ltd.
PII: S0955-2219(02)00293-5

used. Nb_2O_5 was finely ground and was dispersed in 2% aqueous citric acid solution. This was done to prevent the agglomeration of the powder, to some extent, by forming a coating of citric acid on the Nb_2O_5 particles. The solution was continuously stirred using a mechanical stirrer. Aqueous solution of $(NH_4)_2CO_3$ was added in excess followed by a drop-wise addition of aqueous solution of $SrCl_2$ and $BaCl_2$. pH was maintained between 10 and 11. The precipitate was allowed to settle down overnight. No additional precipitation on adding aqueous $(NH_4)_2CO_3$ to the supernatant liquid confirmed the completion of reaction. The precipitate was filtered, washed with water followed by methanol and vacuum dried at room temperature. A flow chart of the partial coprecipitation is shown in Fig. 1. Subsequently the powder was calcined at five different temperatures (900, 1000, 1100, 1150 and 1200 °C). Phillips PW 1729 powder X-ray diffractometer was used for phase analysis. The scan rate of $2\theta = 3°$/min was employed. The particle size and morphology of the powder calcined at 1200 °C was studied using a Phillips CM200 transmission electron microscope at 200 kV. For this, the powder was dispersed using isopropyl alcohol in ultrasonic bath. Few drops of this suspension was taken on a carbon coated copper grid. The calcined powder was ground for an hour and then sintered at 1250, 1300 and 1350 °C for 6, 12 and 24 h, respectively. The density of the sintered pellets was measured by the liquid displacement method using distilled water as displacement fluid following the standard ASTM method.[17] Microstructural studies were carried out using a CAMECA SU 30 SEM probe scanning electron microscope in SE mode. For dielectric measurements, the sintered pellets were gold sputtered (Technics, UK) on both sides and for better contact it was further metallized with silver paste and was oven dried before carrying out dielectric measurements. Solatron SI 1260 impedance analyzer was used to measure the capacitance at 1, 10, 100 KHz and 1 MHz frequencies.

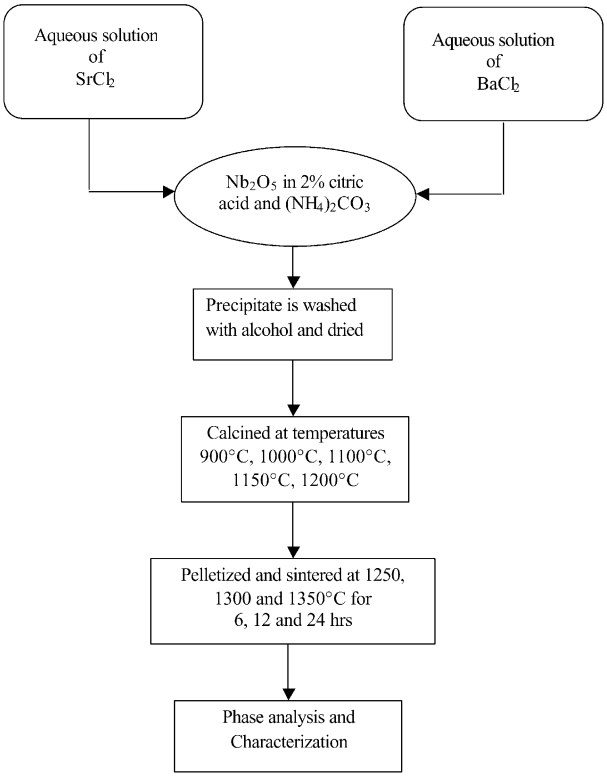

Fig. 1. Flow chart of the partial coprecipitation method.

3. Results and discussion

The X-ray diffraction patterns of powders calcined at different temperatures are shown in Fig. 2(a–e). The diffraction pattern in Fig. 2(a) shows SBN50 phase and

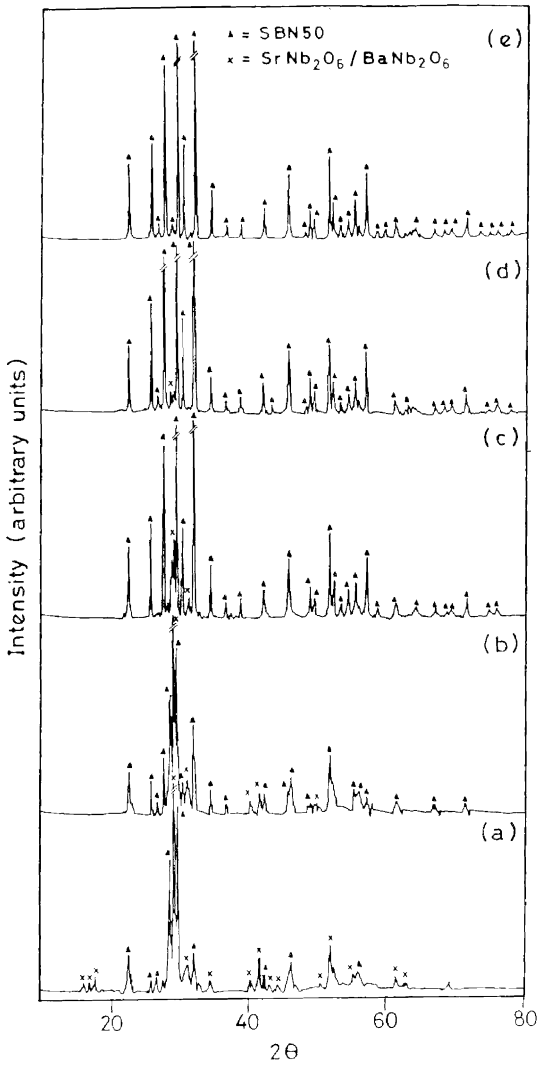

Fig. 2. X-ray diffraction pattern of the powder calcined at (a) 900 °C, (b) 1000 °C, (c) 1100 °C, (d) 1150 °C and (e) 1200 °C. ▲ indicates peak SBN50 phase, × indicates peak of $SrBaNb_2O_6/BaNb_2O_6$ phase.

unreacted phases ($SrNb_2O_6$ and $BaNb_2O_6$), indicating the formation of SBN50 phase at 900 °C. Thermogravimetric analysis of the dried powder showed a weight loss corresponding to loss of CO_2 around 900 °C. The first calcination temperature was therefore chosen at 900 °C. The percentage of SBN50 phase continued to increase untill 1200 °C [Fig. 2(e)], at which 100% SBN50 phase formation occurs as revealed by standard diffraction pattern.[18] It has been reported in the literature that the calcination temperature for SBN50 lies between 1100 and 1200 °C[19,20] when prepared by the conventional solid-state method. Partial coprecipitation method, adopted here for the first time for SBN, also shows complete SBN50 formation at 1200 °C and is therefore consistent with earlier reports.

Fig. 3 shows a typical TEM micrograph of the powder calcined at 1200 °C for 6 h. The size of particles ranged between 250 and 300 nm. TEM observation also showed the presence of high agglomeration in the powder. The particle size for most coprecipitation methods range between 100 and 300 nm.[21,22]

SEM micrographs of the pellets sintered at 1250, 1300 and 1350 °C for 6, 12 and 24 h. are shown in Figs. 4(a–c), 5(a–c), 6(a–c), respectively. Fig. 4(a) show a high porosity in the sample with the grain size between 2 and 8 μm. On closely observing this micrograph it can be seen that the neck formation between the grains has just initiated (first stage of sintering).[23] It may be noted that the grains are irregular in nature and sizes vary widely. However a few grains appear spherical. Fig. 4(b) shows that the grains are more compacted with the grain size ranging between 7 and 15 μm. Grains of 10–15 μm size can be seen in the Fig. 4(c). There does not seem to be appreciable difference in grain character for increase in sintering time from 12 to 24 h at 1250 °C. The grains in Fig. 5(a) appear nicely compacted among themselves but their sizes are varying widely (2–12 μm). In Fig. 5(b) it is observed that the grain sizes are not varying as widely as in Fig. 5(a) with an average size of 10 μm. Fig. 5(c) shows the grains are tetragonal and are elongated in nature. The grain size is varying between 15 and 30 μm. It was observed that the grains were predominantly aligned in one direction as indicated in Fig. 5(c). Tetragonal grains with average grain size of 10 μm can be seen in Fig. 6(a). When sintered at 1350 °C for 12 h. SBN50 shows tetragonal shaped grain structure with an average size of 20 μm [Fig. 6(b)]. On the other hand, when sintered at 1350 °C for 24 h. the grains appear more elongated with average grain size of 30 μm as shown in Fig. 6(c). A comparison of micrographs [Figs. 5(b,c), 6(b,c)] reveals a higher aspect ratio for grains for the sample sintered at 1350 °C than for those sintered at 1300 °C. Abnormal grain growth (~100 μm), has been reported for SBN60 ceramics[3] and similar observations have been made for SBN50, synthesized by conventional solid-state route at authors' laboratory (unreported). The present observations for partial coprecipitated SBN50 reveal unidirectionality in grain growth (maximum 50 μm).

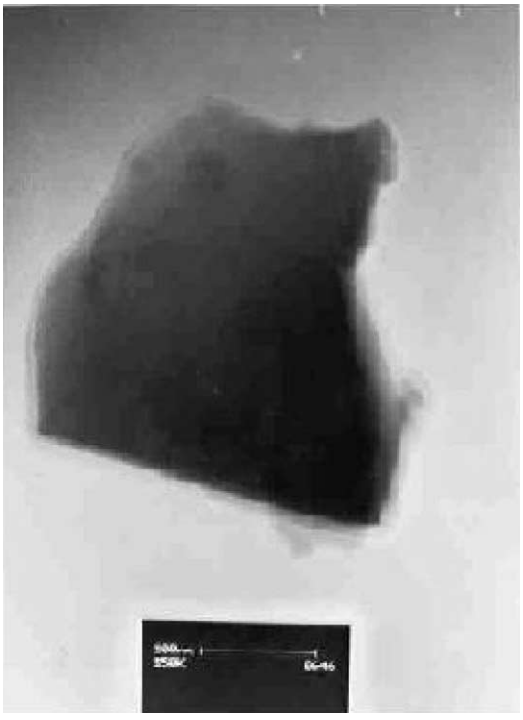

Fig. 3. Transmission electron micrograph of the SBN50 powder calcined at 1200 °C.

Density and porosity have pronounced effect on properties of most electro-ceramics. The density and porosity for SBN50 sintered under different conditions are listed in Table 1. It may be noted that the sample sintered at 1250 °C for 6 h shows density of 4.18 gm/cc [77% of theoretical density (ρ_{Th})]. For other sets of samples the density varied between 89 and 92% of ρ_{Th}, with the exception of sample sintered at 1350 °C for 24 h, which showed a lower density of only 85% of $\rho_{Th.}$ The variation of density between 89 and 92%, is not an appreciable difference since it lies well within the experimental error of density measurements. In general the density increases with both increasing temperature for fixed time and with longer sintering time for fixed temperature. The exceptions arise due to unidirectional grain growth at 1350 °C for 24 h a relatively longer sintering cycle and inadequate sintering at 1250 °C for 6 h. The increase in porosity at 1350 °C for 24 h. may be attributed to the typical tetragonal shape of the grains that resulted in relatively loose packing of grains and increase in open pore size because of Ostwald ripening of pores. The microstructures illustrated in Figs. 4(a) and 6(c) clearly substantiate above observations. Therefore, it may be inferred that increase in time of sintering only resulted in the increase of grain size but did not contribute to enhancement in density due to abnormal grain growth in one direction. The variation

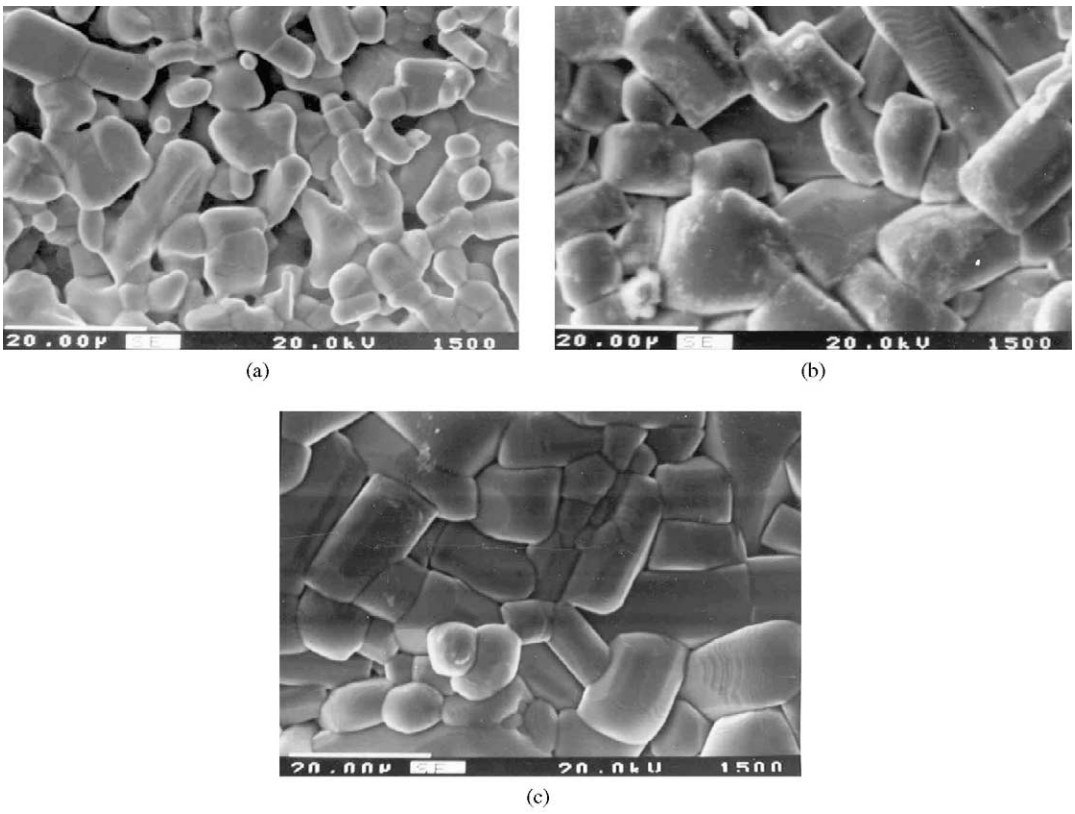

Fig. 4. Scanning electron micrograph of the sample sintered at 1250 °C for (a) 6, (b) 12 and (c) 24 h.

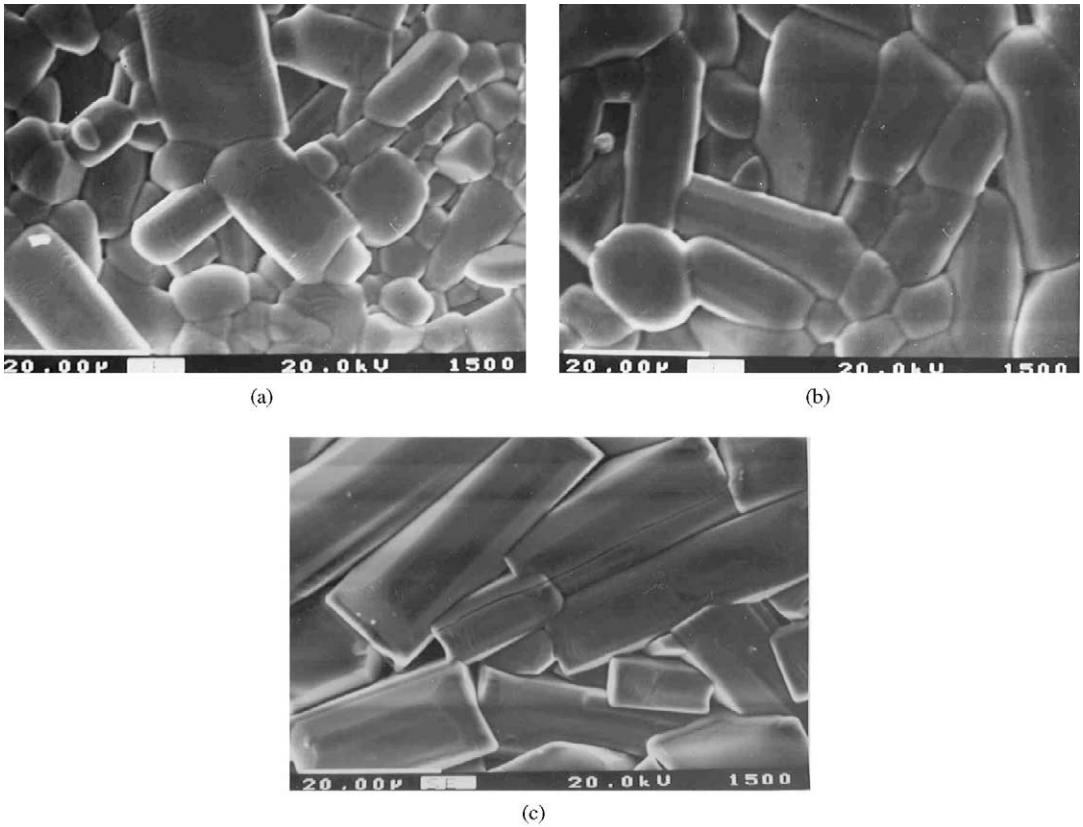

Fig. 5. Scanning electron micrograph of the sample sintered at 1300 °C for (a) 6, (b) 12 and (c) 24 h.

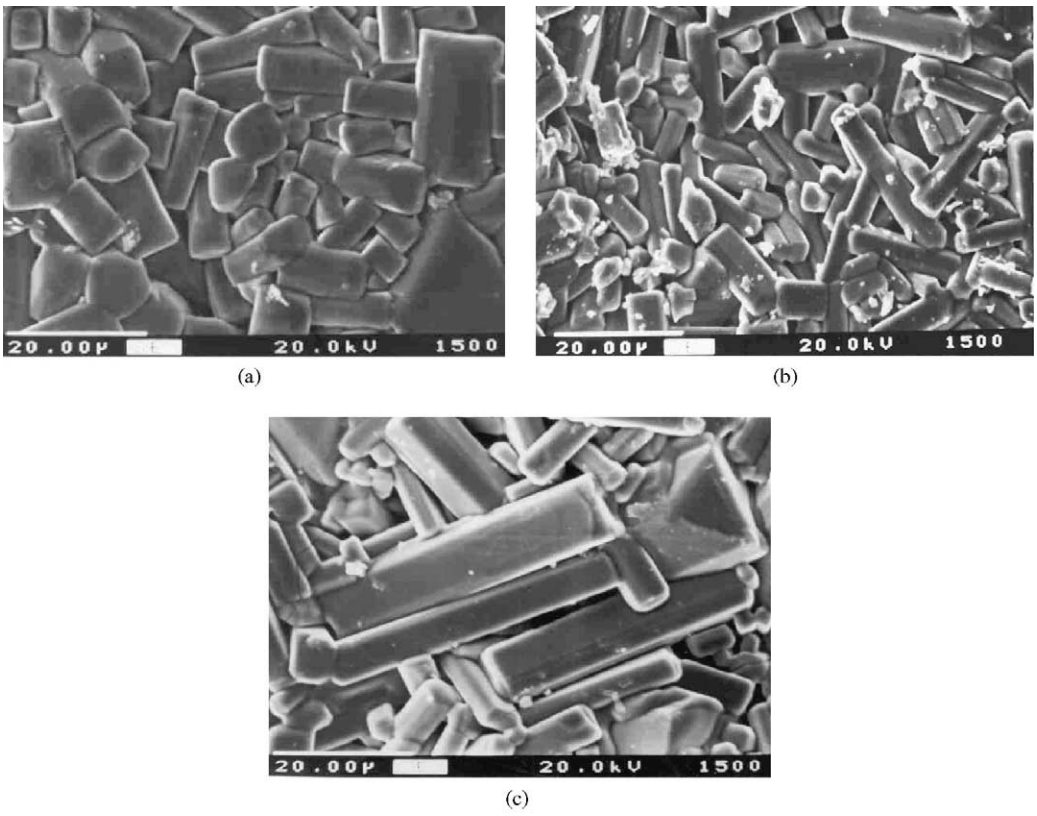

Fig. 6. Scanning electron micrograph of the sample sintered at 1350 °C for (a) 6, (b) 12 and (c) 24 h.

of density with temperature for a fixed time and the variation of density with time for fixed temperature are shown in the Fig. 7(a) and (b).

A typical variation of dielectric constant (corrected for porosity) with temperature for SBN50 sintered at 1350 °C for different times is shown in Fig. 8(a–c). Similar results were observed for all other sintering conditions. Porosity correction was made using Rushman and Strivens equation.[24]

Table 1
Variation of density and porosity of SBN50 sintered under different conditions

Sintering temp (°C)	Soaking time (h)	Density measured (gm/cc)	% Of theoretical density (ρ_{Th} = 5.42 gm/cc)	Porosity in % (Open pores + Closed pores) (100-%ρ_{Th})
1250	6	4.18	77.12	22.88
1250	12	4.93	90.95	9.05
1250	24	4.98	91.88	8.12
1300	6	4.83	89.11	10.89
1300	12	4.88	90.03	9.97
1300	24	5.00	92.25	7.75
1350	6	4.94	91.15	8.85
1350	12	4.90	90.40	9.60
1350	24	4.62	85.24	14.76

$$\varepsilon_{\text{corrected}} = \frac{\varepsilon_{\text{observed}} \times (2 + V_2)}{2(1 - V_2)}$$

where V_2 is the volume fraction of porosity in the sintered compact.

In all the cases a broad peak, characteristic of relaxor is observed. Maximum dielectric constant observed (ε_{max}) at 1 KHz and T_c for SBN50 sintered under different conditions is listed in Table 2. From the table, it may be noted that at 1250 °C, ε_{max} increases from 830 to 1453 while T_c varies between 94 and 90 °C as the sintering time increases. Similarly at 1300 °C the ε_{max} are 1249, 1284 and 1244 at the corresponding T_c of 96 °C, 119 and 113 °C, when the sintering time increases from 6 to 24 h. The ε_{max} steadily decreases from 1611 to 1219 and the corresponding T_c varies between 95 and 93 °C. It is clear that, for the set sintered at 1250 °C for different durations there is a steady increase in ε_{max} with time and this is due to increase in grain size. For the set sintered at 1300 °C, there is almost no change in ε_{max}. However at 1350 °C, there is a steady decrease in the ε_{max} with increase in time of sintering. This variation in dielectric constant is in agreement with the variation in density.

The observed dielectric constants are consistent with the reported values (ε_{max} ~1585) for SBN50 synthesized by solid-state methods.[9] But few other groups have reported higher dielectric constants, for example

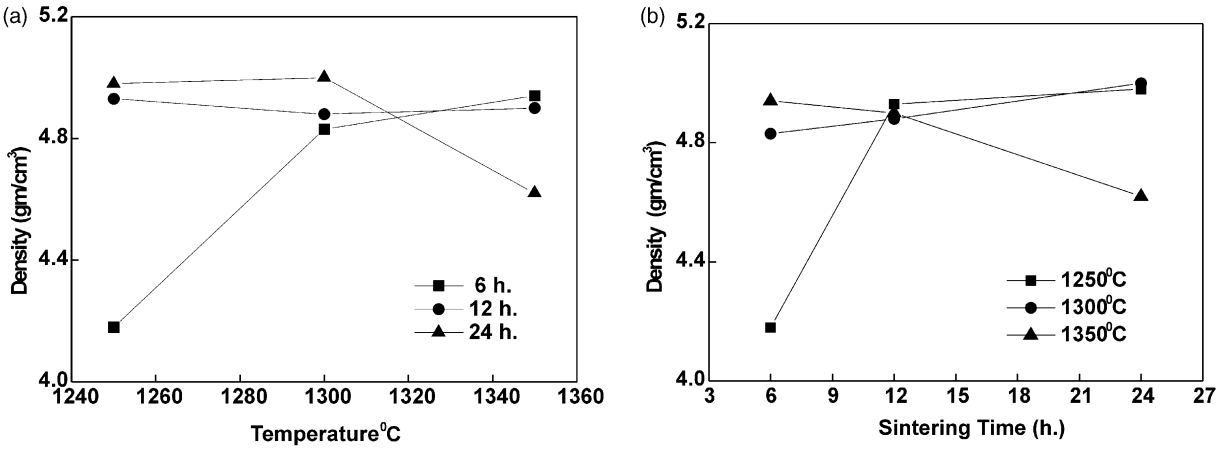

Fig. 7. (a) Variation of density with temperature at fixed time of sintering; (b) variation of density with time at fixed temperature of sintering.

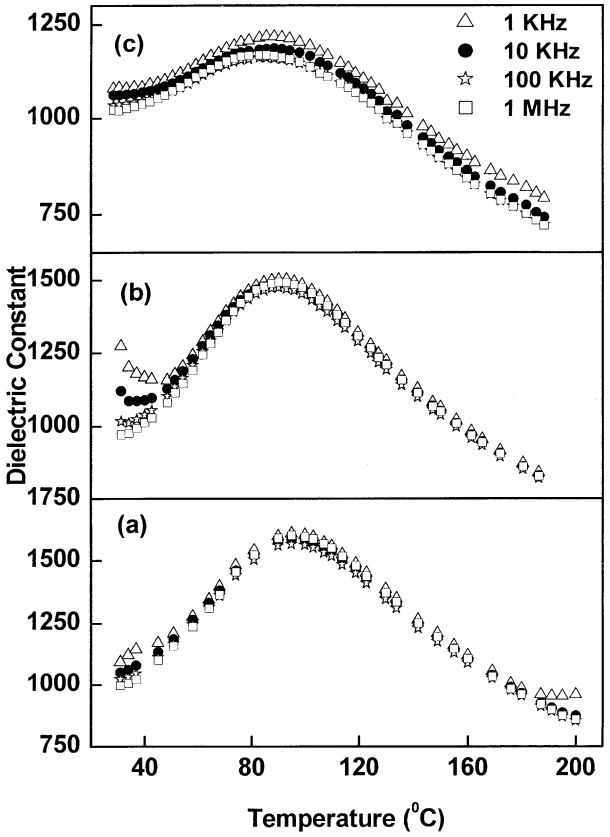

Fig. 8. Dielectric constant versus temperature plot of sample sintered at 1350 °C for (a) 6, (b) 12 and (c) 24 h.

2150[11] and ~3750,[25] when compared with the observed data. Variation in T_c, from 90 to 119 °C agrees well with the reported values of T_c for SBN50 composition [~80 °C,[11] 119 °C,[9] 50–55 °C and 80–90 °C[25]]. The variation in T_c for the same SBN50 composition remains an unresolved issue. A detailed study to understand these variations has been undertaken and would be reported separately.

Table 2
Dielectric constant and Curie temperature (T_c) for SBN50 sintered under different conditions

Sample	Density (gm/cc)	$T_{porosity}$	T_c (°C)	ε_{max} at 1 KHz (observed)	ε_{max} at 1 KHz (corrected)
1250 °C, 6 h	4.18	22.88	94	574	830
1250 °C, 12 h	4.93	9.05	94	1146	1317
1250 °C, 24 h	4.98	8.12	90	1283	1453
1300 °C, 6 h	4.83	10.89	96	1107	1249
1300 °C, 12 h	4.88	9.97	119	1100	1282
1300 °C, 24 h	5.00	7.75	113	1105	1244
1350 °C, 6 h	4.94	8.85	95	1406	1611
1350 °C, 12 h	4.90	9.60	95	1299	1505
1350 °C, 24 h	4.62	14.76	93	968	1219

4. Conclusion

Strontium barium niobate has been synthesized, for the first time, using the partial coprecipitation method. Sintering conditions have been optimized. A high ε (1611) has been observed for sample sintered at 1350 °C for 6 h. The highest density achieved has been ~92% of the theoretical density. Sintering temperature has more pronounced effect on dielectric constant than sintering time. In conclusion, partial coprecipitation has been shown as an alternate route for synthesis of SBN, an important ferroelectric material. It is expected that materials synthesized through this method would exhibit superior homogeneity since two components of the three component systems are in solution state and coprecipitation was done on fine Nb_2O_5 particles. An additional advantage is that sub-micron sized powders have been synthesized while eliminating grinding steps, which, otherwise, are mandatory for solid-state process. Furthermore, abnormal grain growth in SBN, which is often a matter of concern with the solid-state process, has been suppressed in the current approach. The unidirectional grain growth in the material associated with

long sintering cycles in the present synthesis method, gives an opportunity for the possibility of texturising the material in a preferred axis of easy polarization, which in-turn, will increase the dielectric and ferroelectric properties of the material. This will further increase the potential application of the material for device fabrication.

Acknowledgements

Access to SEM and TEM facility provided by RSIC, IIT-Bombay, is gratefully acknowledged.

References

1. Trubelja, M. P., Ryba, E. and Smith, D. K., A study of positional disorder in strontium barium niobate. *J. Mat. Sci.*, 1996, **31**, 1435–1443.
2. Heartling, G. H. and Land, C. E., Hot pressed (Pb,La)(Zr,Ti)O_3 ferroelectric ceramic for electro-optic applications. *J. Am. Ceram. Soc.*, 1971, **54**, 1–11.
3. Antisigin, V. D., Kotsov, E. G., Malinovsky, V. K. and Sterelyukhina, L. N., Electrooptics of thin ferroelectric films. *Ferroelectrics*, 1981, **38**, 761–763.
4. Neurgaonkar, R. R., Oliver, R. and Cory, W. K., Piezoelectricity in tungsten bronze crystals. *Ferroelectrics*, 1994, **160**, 265–276.
5. Neurgaonkar, R. R. and Cross, L. E., Piezoelectric tungsten bronze crystals for SAW device applications. *Mat. Res. Bull.*, 1986, **21**, 893–899.
6. Glass, A. M., Investigation of electrical properties of $Sr_{1-x}Ba_xNb_2O_6$ with special reference to pyroelectric detection. *J. Appl. Phys.*, 1969, **40**, 4699–4713.
7. Ewbank, M. D., Neurgaonkar, R. R., Cory, W. K. and Feinberg, J., Photo-refractrive properties of strontium barium niobate. *J. Appl. Phys.*, 1987, **62**, 374–380.
8. Rytz, D., Wechsler, B. A., Schwartz, R. N., Nelson, C. C., Brandle, C. D., Valentino, A. J. and Berkstresser, G. W., Temperature dependence of photorefractive properties of strontium barium niobate ($Sr_{0.6}Ba_{0.4}Nb_2O_6$). *J. Appl. Phys.*, 1989, **66**, 1920–1924.
9. Vandamme, N. S., Sutherland, A. E., Jones, L., Bridger, K. and Winzer, S. R., Fabrication of optically transparent and electro-optic strontium barium niobate ceramics. *J. Am. Ceram. Soc.*, 1994, **74**, 1785–1792.
10. Fang, T., Wu, N. and Shiau, F., Formation mechanism of strontium barium niobate ceramic powders. *J. Mat. Sci. Lett.*, 1994, **13**, 1746–1748.
11. Deshpande, S. B., Potdar, H. S., Godbole, P. D. and Date, S. K., Preparation and ferroelectric properties of SBN:50 ceramics. *J. Am. Ceram. Soc.*, 1992, **75**, 2581–2585.
12. Nishiwaki, S., Takahashi, J. and Kodaira, K., Effect of additives on microstructure development and ferroelectric properties of $Sr_{0.3}B_{0.7}Nb_2O_6$ ceramics. *Jpn. J. Appl. Phys.*, 1994, **33**, 5477–5481.
13. Hirano, S., Yogo, T., Kikuta, K. and Ogiso, K., Preparation of strontium barium niobate by sol-gel method. *J. Am. Ceram. Soc.*, 1992, **75**, 1697–1700.
14. Xu, Y., Chen, J., Xu, R. and Mackenzie, J. D., Ferrroelectric $Sr_{0.6}Ba_{0.4}Nb_2O_6$ thin film by the sol-gel process: electrical and optical properties. *Phy. Rev. B*, 1991, **44**, 35–41.
15. Lu, S. G., Mak, C. L. and Wong, K. H., Low temperature preparation and size effect of strontium barium niobate ultrafine powder. *J. Am. Ceram. Soc.*, 2001, **84**, 79–84.
16. Panda, A. B., Pathak, A. and Pramanik, P., Low temperature preparation of nanocrystalline solid solution of strontium-barium-niobate by chemical process. *Mat. Lett.*, 2002, **52**, 180–186.
17. *Annual Book of ASTM standards*, 1916 Race Street, PA, 1989, 15, C373–88, pp. 109–110.
18. Joint Committee on powder diffraction standards, 1601 Park Lane, Swarthmare, Pensylvania 19081, Catalogue No 39–0265.
19. Qua, Y. Q., Li, A. D., Shao, Q. Y., Tang, Y. F., Wu, D., Mak, C. L., Wong, K. H. and Ming, N. B., Structure and electrical properties of strontium barium niobate ceramics. *Mat. Res. Bull.*, 2002, **37**, 503–513.
20. Fang, T. T., Chen, E. and Lee, W. J., On the discontinuous grain growth of $Sr_xBa_{1-x}Nb_2O_6$ ceramics. *J. Eur. Ceram. Soc.*, 2000, **20**, 527–530.
21. Popa, M., Totovana, A., Popescu, L., Dragan, N. and Zaharescu, M., Reactivity of the Bi, Sr, Ca, Cu oxalate powders used in BSCCO preparation. *J. Eur. Ceram. Soc.*, 1998, **18**, 1265–1271.
22. Zang, Y., Lin, Y. S. and Swartz, S. L., Perovskite-type ceramic membrane: synthesis, oxygen permeation and membrane reactor performance for oxidative coupling of methane. *J. Mem. Sci.*, 1990, **150**, 87–98.
23. German, R. M., *Sintering Theory and Practice*. John Wiley Publication, New York, 1996.
24. Rushman, D. F. and Strivens, M. A., The effective permittivity of two phase system. *Proc. Phys. Soc.*, 1947, **59**, 1011–1016.
25. Jimenez, B., Alemany, C. and Mendiola, J., Phase transitions in ferroelectric ceramics of the type $Sr_{0.5}Ba_{0.5}Nb_2O_6$. *J. Phys. Chem. Solids*, 1985, **45**, 1383–1386.